Prioritization-based constrained trajectory planning for a nonlinear turbocharged air system with EGR

authored by **P. Kotman, M. Bitzer, and A. Kugi**

and published in *Proccedings of the American Control Conference (ACC)*.

Cite this article as:

P. Kotman, M. Bitzer, and A. Kugi, "Prioritization-based constrained trajectory planning for a nonlinear turbocharged air system with EGR", in *Proccedings of the American Control Conference (ACC)*, Montreal, Canada, Jun. 2012, pp. 5712–5717

BibTex entry:

```
@inproceedings{Kotman2012,
  author = {Kotman, P. and Bitzer, M. and Kugi, A.},
  title = {{Prioritization-based constrained trajectory planning for a nonlinear turbocharged air system
      with EGR}},
  booktitle = {Proccedings of the American Control Conference (ACC)},
  month = {jun 27-29},
  year = {2012},
  address = {Montreal, Canada},
  pages = {5712--5717}
}
```

Link to original paper:

Contact:

Automation and Control Institute (ACIN)
Vienna University of Technology
Gusshausstrasse 27-29/E376
1040 Vienna, Austria

Internet: www.acin.tuwien.ac.at
E-mail: office@acin.tuwien.ac.at
Phone: +43 1 58801 37601
Fax: +43 1 58801 37699

Prioritization-Based Constrained Trajectory Planning for a Nonlinear Turbocharged Air System with EGR

Philipp Kotman, Matthias Bitzer, and Andreas Kugi

***Abstract*— The problem of generating sufficiently smooth reference trajectories for the flatness-based feedforward control of a Diesel engine air system with input constraints is addressed in this work. The proposed trajectory planning can handle arbitrary command inputs and provides the reference signals required by the flatness-based controller. Thereby, the desired tracking behavior for the controlled variables is defined by a linear target system. The input constraints are taken into account by limiting the target system dynamics to the realizable air system dynamics as determined by the flat design model and the limits of the control input. Furthermore, a prioritization of the controlled variables is included in this limitation. The differentially flat reduced-order design model used in this work is deduced from a high-order reference model by applying the singular perturbation theory. The suitability of the proposed trajectory planning in combination with the feedforward controller is shown by means of simulation studies relying on the high-order reference air system model.**

I. Introduction

Today, internal combustion engines (ICEs) usually ought to meet different requirements. While consumers demand for high power and economy, legislators mainly stipulate low pollutant emissions. A prevalent means of simultaneously increasing power and reducing emissions are exhaust-driven turbochargers as they improve the ICE efficiency. The basic idea of turbocharging is to use the energy of the exhaust-gas to boost the pressure at the engine's intake. Additionally, an exhaust-gas recirculation (EGR) is often used to lower the nitrogen oxide (NOx) emissions [1]. The one-stage air system with wastegate turbocharger and high-pressure EGR considered here is discussed in detail in Sec. II.

The control problem related to the turbocharged air system with EGR is a nonlinear multivariable control problem [2], [3], [4]. As in most real-world problems [5], [6], the available control inputs feature constraints [2], [7], [8] significantly limiting the achievable control performance in terms of tracking fast reference trajectories. Neglecting these constraints almost unavoidably leads to performance degradation [9], may induce changes of the direction of the applied control [10], [11], or can even cause instability [6], [9], [12].

Many concepts for turbocharged air system control with EGR are presented in the literature, including constructive Lyapunov [13], sliding mode [14], fuzzy [15], and linear parameter-varying control [16], as well as feedback linearization [4], where input constraints are not taken into account systematically. In contrast to that, the use of classical anti-windup measures is reported in [2] and a constrained motion planning is employed in [8] to ensure the adherence to input constraints. Furthermore, model predictive control methods easily deal with different types of constraints [3], [17].

Fig. 1. Setup used for air system control.

In this work, a nonlinear flatness-based [18] multivariable feedforward (FF) controller first presented in [19] is used for air system (AS) control. The input constraints are included into the control setup depicted in Fig. 1 by combining the FF controller with a target-system-based trajectory planning (TP) that explicitly respects the constraints. The desired tracking behavior from the command input y^{d} to the air system output y is defined by a linear target system, also referred to as reference model in the literature [20], [21]. For the corresponding control input u computed by the FF controller to strictly comply with the input constraints, the dynamics of the target system has to be restricted. To this end, the constraints on the control input are transformed into the required constraints on the target system dynamics using the flat air system model also utilized for control design. The resulting limited target system is a switched nonlinear system serving as the desired TP, i.e. it takes arbitrary command inputs y^{d} and generates a sufficiently smooth reference signal w that can be followed by the air system output y in the absence of disturbances and model uncertainties. Finally, the symbol $w^{[r]}$ denotes the vector of the reference w and its time derivatives as required by the flatness-based FF controller.

Both, the FF controller and the TP, are developed on the basis of a differentially flat reduced-order model (ROM) of the air system, which is deduced from a high-order reference model in Sec. II. The differential flatness of the nonlinear ROM is shown and the FF controller is obtained by means of the respective input parametrization in Sec. III. The TP is developed as a linear target system with prioritization-based limitation in Sec. IV. The suitability of the proposed approach is evaluated by means of simulation studies in Sec. V, before the summary in Sec. VI concludes this work.

II. The Turbocharged Air System

An introduction to the turbocharged air system with EGR is given in this section. Its working principle is discussed in Sec. II-A, followed by the formulation of the related control problem in Sec. II-B. The ROM utilized for the design of the FF controller and the TP is presented in Sec. II-C.

P. Kotman and M. Bitzer are with the Control Engineering Group, Corporate Sector Research, Robert Bosch GmbH, Stuttgart, Germany {philipp.kotman,matthias.bitzer2}@de.bosch.com

A. Kugi is with the Automation and Control Institute, Vienna University of Technology, Vienna, Austria kugi@acin.tuwien.ac.at

Post-print version of the article: P. Kotman, M. Bitzer, and A. Kugi, "Prioritization-based constrained trajectory planning for a nonlinear turbocharged air system with EGR", in *Proccedings of the American Control Conference (ACC)*, Montreal, Canada, Jun. 2012, pp. 5712–5717

The content of this post-print version is identical to the published paper but without the publisher's final layout or copy editing.

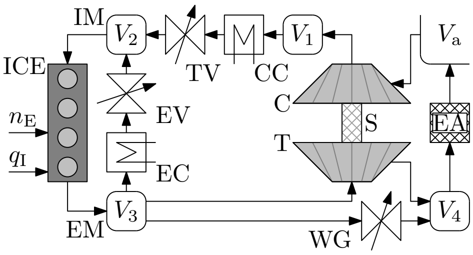

Fig. 2. Sketch of the turbocharged Diesel air system with EGR [19].

A. *System Description*

The efficiency of the overall engine system is improved using a charge-air cooler (CC) and an EGR cooler (EC). Hence, the working principle of the air system depicted in Fig. 2 is as follows. Fresh air is aspirated from the ambiance V_a (with constant pressure p_a and temperature T_a), compressed by the compressor (C), led into the piping section V_1, cooled by the CC, passes the throttle valve (TV), is mixed with exhaust gas in the intake manifold (IM) V_2, and then induced into the cylinders of the ICE. Thereby, the engine's behavior is mainly determined by the engine speed n_E, the injected fuel mass q_I, and the pressure p_2 in the IM. Hot exhaust gas is exhaled into the exhaust manifold (EM) V_3 and partly fed back into the IM via the EC and the EGR valve (EV). The remaining exhaust gas drives the turbine (T), which in turn powers the compressor (C) via the shaft (S). The wastegate (WG) is used to by-pass the turbine at high engine speed and torque. The burned gas finally leaves the air system through the exhaust aftertreatment.

B. *Problem Formulation*

The air system variables that have to be adjusted to achieve a desired combustion behavior are the boost pressure p_2 and the EGR rate r_E, i.e. the mass fraction of exhaust gas in the IM. The available control inputs are the cross-sectional areas u_E and u_W of the EV and the WG used to manipulate the corresponding mass flows $\dot{m}_\mathrm{EV}$ and $\dot{m}_\mathrm{WG}$. Thereby, all inputs are constrained by physical limits, i.e.

$$u = [\, u_\mathrm{E} \,,\, u_\mathrm{W} \,]^\mathrm{T} \in \mathcal{U} = \mathcal{U}_\mathrm{E} \times \mathcal{U}_\mathrm{W} \subset \mathbb{R} \times \mathbb{R} \qquad (1)$$

with $\mathcal{U}_i = \{u_i \,|\, 0 \leq u_i \leq \overline{u}_i\}$, $i \in \{\mathrm{E}, \mathrm{W}\}$, which imposes significant restrictions for the control design. Finally, the TV is not used for control here and is thus entirely opened.

The combined EGR rate and boost pressure control problem is solved by means of a flatness-based FF controller [19] in this work. For high tracking performance it is combined with a TP that explicitly accounts for the input constraints $u \in \mathcal{U}$ according to (1). The goal of this work is to design the TP in such a way that the FF controlled air system achieves excellent performance in terms of tracking of fast EGR rate and boost pressure reference trajectories.

C. *Air System Modeling*

Following a modular approach, the air system can be described by a high-order nonlinear ordinary differential equation (ODE) model [22], which is further used as a reference for the evaluation of the ROM, the FF controller, and the TP. Due to the complexity of this full-order model (FOM), a ROM has to be derived for control design. Since the pressure and temperature dynamics in the plenum chambers are considerably faster than the rotational dynamics of the shaft S, the singular perturbation theory [23] can be applied to reduce the state dimension of the FOM [19].

For the singular perturbation theory to lead to a differentially flat ODE model, further simplifications have to be employed [19]. In particular, simplified models for e.g. the turbine and the compressor are defined, the temperature T_2 in the IM is assumed to be constant, and the controlled variables $r_\mathrm{E} = p_2^\mathrm{e}/p_2$ and $p_2 = p_2^\mathrm{e} + p_2^\mathrm{f}$ are approximated on the basis of the partial pressures p_2^e and p_2^f of exhaust gas and fresh air in the IM. The ROM thus takes the form [19]

$$\frac{\mathrm{d}p_2^\mathrm{e}}{\mathrm{d}t} = k_2\big(\dot{m}_\mathrm{EV}(x,u,\theta) - K_\mathrm{E}(\theta)p_2^\mathrm{e}\big) \qquad = f_2^\mathrm{e}(x,u,\theta) \quad (2a)$$

$$\frac{\mathrm{d}p_2^\mathrm{f}}{\mathrm{d}t} = k_2\big(\dot{m}_\mathrm{TV}(x) - K_\mathrm{E}(\theta)p_2^\mathrm{f}\big) \qquad = f_2^\mathrm{f}(x,\theta) \quad (2b)$$

$$\frac{\mathrm{d}\omega_\mathrm{S}}{\mathrm{d}t} = \frac{k_\mathrm{S}}{\omega_\mathrm{S}}\big(P_\mathrm{T}(x,u,\theta) - P_\mathrm{C}(x) - P_\mathrm{F}(x)\big) = f_\mathrm{S}(x,u,\theta) \quad (2c)$$

$$y = \big[\, p_2^\mathrm{e} \;\; p_2^\mathrm{f} \,\big]^\mathrm{T}, \;\; x = \big[\, p_2^\mathrm{e} \;\; p_2^\mathrm{f} \;\; \omega_\mathrm{S} \,\big]^\mathrm{T}, \;\; x(0) = x_0 \quad (2d)$$

with the engine parameters $\theta = [n_\mathrm{E}, q_\mathrm{I}]^\mathrm{T}$, the constants $k_2 = (RT_2)/V_2$ and $k_\mathrm{S} = 1/J_\mathrm{S}$, the gas constant R, the volume V_2 of the IM, the moment of inertia J_S of the shaft, and the parameter $K_\mathrm{E}(\theta)$ of a mean-value engine model [22]. The mass flows through the EV and the TV read as

$$\dot{m}_\mathrm{EV}(x,u,\theta) = \frac{v_\mathrm{E}(\dot{m}_\mathrm{E} v_\mathrm{W} + a_\mathrm{EA}(\dot{m}_\mathrm{E} - v_\mathrm{W}\Delta p_\mathrm{a}))}{v_\mathrm{E} v_\mathrm{W} + a_\mathrm{EA}(v_\mathrm{E} + v_\mathrm{W})}, \quad (3a)$$

$$\text{and} \quad \dot{m}_\mathrm{TV}(x) = \frac{a_\mathrm{TV}(a_\mathrm{C}\omega_\mathrm{S} p_\mathrm{a} - b_\mathrm{C}(\omega_\mathrm{S}' - \omega_\mathrm{S})\Delta p_\mathrm{a})}{a_\mathrm{TV} + b_\mathrm{C}(\omega_\mathrm{S}' - \omega_\mathrm{S})}, \quad (3b)$$

with the auxiliary inputs $v_\mathrm{E} = a_\mathrm{EV} u_\mathrm{E}$ and $v_\mathrm{W} = a_\mathrm{T} - b_\mathrm{T}\omega_\mathrm{S} + c_\mathrm{T} u_\mathrm{W}$, the pressure difference $\Delta p_\mathrm{a} = p_2 - p_\mathrm{a}$, the mass flow $\dot{m}_\mathrm{E} = K_\mathrm{E}(\theta)p_2 + \dot{m}_\mathrm{F}(\theta)$ into the EM, and the fuel mass flow $\dot{m}_\mathrm{F}(\theta)$. The constant parameters a_TV, a_EV, a_EA, a_C, b_C, ω_S', a_T, b_T, and c_T stem from the simplified models of the TV, the EV, the EA, the C, and the T [19], respectively. The time derivative of the shaft speed ω_S (2c) is influenced by the friction power $P_\mathrm{F}(x) = d_\mathrm{S}\omega_\mathrm{S}^2$, as well as the turbine power $P_\mathrm{T}(x,u,\theta)$, and the compressor power $P_\mathrm{C}(x)$, given by

$$P_\mathrm{T}(x,u,\theta) = \frac{a_\mathrm{EA}\bar{\eta}_\mathrm{T}(\dot{m}_\mathrm{E} + v_\mathrm{E}\Delta p_\mathrm{a})\Theta_\mathrm{L}\dot{H}_\mathrm{TC}}{a_\mathrm{EA} v_\mathrm{E} v_\mathrm{W} + (\dot{m}_\mathrm{E} + v_\mathrm{E} p_2 + a_\mathrm{EA} p_\mathrm{a}) v_\mathrm{W}^2}, \quad (3c)$$

$$P_\mathrm{C}(x) = \frac{\bar{\eta}_\mathrm{C}(a_\mathrm{C}\omega_\mathrm{S} p_\mathrm{a} + a_\mathrm{TV}\Delta p_\mathrm{a})\dot{H}_\mathrm{a}}{(a_\mathrm{TV} + b_\mathrm{C}(\omega_\mathrm{S}' - \omega_\mathrm{S}))p_\mathrm{a}}, \quad (3d)$$

where the parameters $\bar{\eta}_\mathrm{C}$ and $\bar{\eta}_\mathrm{T}$ stem from the simplified models of the C and the T, respectively, d_S is the friction damping coefficient of the bearing, and $\Theta = a_\mathrm{T} - b_\mathrm{T}\omega_\mathrm{S}$. The quantities $\dot{m}_\mathrm{TC} = \dot{m}_\mathrm{E} - \dot{m}_\mathrm{EV}$ and $\dot{H}_\mathrm{TC} = \dot{m}_\mathrm{TC} c_\mathrm{p} T_3$ are the mass and enthalpy flow used for turbocharging and $\dot{H}_\mathrm{a} = \dot{m}_\mathrm{TV} c_\mathrm{p} T_\mathrm{a}$ is the fresh-air enthalpy flow, where c_p is the isobaric heat capacity and the temperature T_3 is described by the phenomenological model given in [22]. Finally, note that here and in the sequel the dependencies on the state x, the input u, and the parameter θ are omitted for brevity.

Post-print version of the article: P. Kotman, M. Bitzer, and A. Kugi, "Prioritization-based constrained trajectory planning for a nonlinear turbocharged air system with EGR", in *Proccedings of the American Control Conference (ACC)*, Montreal, Canada, Jun. 2012, pp. 5712–5717
The content of this post-print version is identical to the published paper but without the publisher's final layout or copy editing.

III. Flatness-Based Feedforward Control

In this section, the design of the flatness-based FF air system controller according to [19] is summarized. By deriving the corresponding state and input parametrization in Sec. III-A and III-B, respectively, it is shown that the output y (2d) constitutes a flat output [24] of the ROM (2).

A. State Parametrization

The parametrization of the state x (2d) in terms of the flat output y (2d) and its time derivatives is given next. The first two components of the state x are parametrized by [19]

$$p_2^{\mathrm{e}} = y_1, \quad p_2^{\mathrm{f}} = y_2, \tag{4a}$$

where y_1 and y_2 are the two components of the flat output y. The parametrization of the shaft speed ω_{S} is obtained from $\mathrm{d}y_2/\mathrm{d}t = \mathrm{d}p_2^{\mathrm{f}}/\mathrm{d}t = f_2^{\mathrm{f}}(x,\theta)$, cf. (2b), leading to [19]

$$\omega_{\mathrm{S}} = \frac{(a_{\mathrm{TV}}+b_{\mathrm{C}}\omega_{\mathrm{S}}')\Xi + a_{\mathrm{TV}} b_{\mathrm{C}} k_2 \Delta p_{\mathrm{a}} \omega_{\mathrm{S}}'}{a_{\mathrm{TV}} k_2 (a_{\mathrm{C}} p_{\mathrm{a}} + b_{\mathrm{C}} \Delta p_{\mathrm{a}}) + b_{\mathrm{C}} \Xi} \tag{4b}$$

with $\Xi = k_2 K_{\mathrm{E}} y_2 + \mathrm{d}y_2/\mathrm{d}t$. The nonlinear transformation

$$z = \left[\, z_1 \;\; z_2 \;\; z_3 \,\right]^{\mathrm{T}} = \left[\, p_2^{\mathrm{e}} \;\; p_2^{\mathrm{f}} \;\; f_2^{\mathrm{f}} \,\right]^{\mathrm{T}} = \Phi(x) \tag{5}$$

hence proves to be a diffeomorphism, i.e. the inverse mapping $x = \Phi^{-1}(z)$ given by (4) exists and is smooth as well.

B. Input Parametrization

With the state parametrization (4), the input parametrization is obtained from the r-th order time derivatives

$$\frac{\mathrm{d}y_1}{\mathrm{d}t} = k_2\big(\dot m_{\mathrm{EV}} - K_{\mathrm{E}} y_1\big) \qquad = \gamma_1(x,u) \tag{6a}$$

$$\frac{\mathrm{d}^2 y_2}{\mathrm{d}t^2} = \overbrace{\frac{\partial f_2^{\mathrm{f}}}{\partial p_2^{\mathrm{e}}}\frac{\mathrm{d}y_1}{\mathrm{d}t} + \frac{\partial f_2^{\mathrm{f}}}{\partial p_2^{\mathrm{f}}}\frac{\mathrm{d}y_2}{\mathrm{d}t} + \frac{\partial f_2^{\mathrm{f}}}{\partial \theta}\frac{\mathrm{d}\theta}{\mathrm{d}t}}^{=\Lambda} + \frac{k_{\mathrm{S}}}{\omega_{\mathrm{S}}}\frac{\partial f_2^{\mathrm{f}}}{\partial \omega_{\mathrm{S}}}\big(P_{\mathrm{T}} - P_{\mathrm{C}} - P_{\mathrm{F}}\big) \qquad = \gamma_2(x,u), \tag{6b}$$

of the flat output y, where $r = [1,2]^{\mathrm{T}}$ is the system's vector relative degree [24]. Henceforth, $\gamma = [\,\mathrm{d}y_1/\mathrm{d}t\,,\, \mathrm{d}^2y_2/\mathrm{d}t^2\,]^{\mathrm{T}}$ is referred to as the r-derivative of the output y. Equations (6) are solved for the only input-dependent quantities, i.e.

$$\dot m_{\mathrm{EV}} = \gamma_1/k_2 + K_{\mathrm{E}} y_1, \tag{7a}$$

$$P_{\mathrm{T}} = P_{\mathrm{C}} + P_{\mathrm{F}} + \left(\frac{k_{\mathrm{S}}}{\omega_{\mathrm{S}}}\frac{\partial f_2^{\mathrm{f}}}{\partial \omega_{\mathrm{S}}}\right)^{-1}\big(\gamma_2 - \Lambda\big), \tag{7b}$$

where the inverse in (7b) is guaranteed to exist for all admissible operating points of the air system. In the next step, the control inputs u_{E} and u_{W} are computed from (3a) and (3c). For the EGR valve actuation u_{E} this yields [19]

$$u_{\mathrm{E}} = \frac{a_{\mathrm{EA}} \dot m_{\mathrm{EV}} v_{\mathrm{W}}}{a_{\mathrm{EV}}\big((a_{\mathrm{EA}} + v_{\mathrm{W}})\dot m_{\mathrm{TC}} - a_{\mathrm{EA}} v_{\mathrm{W}} \Delta p_{\mathrm{a}}\big)}. \tag{8a}$$

Using (8a), the turbine power P_{T} (3c) is rearranged to

$$v_{\mathrm{W}}^2 = \frac{\Psi \Theta \dot H_{\mathrm{TC}}}{\Upsilon P_{\mathrm{T}}},$$

which is finally solved for the wastegate actuation [19]

$$u_{\mathrm{W}} = -\frac{\Theta}{c_{\mathrm{T}}} \pm \sqrt{\frac{\Psi \Theta \dot H_{\mathrm{TC}}}{c_{\mathrm{T}}^2 \Upsilon P_{\mathrm{T}}}}, \tag{8b}$$

where $\Psi = a_{\mathrm{EA}} \bar\eta_{\mathrm{T}} \dot m_{\mathrm{TC}}$ and $\Upsilon = \dot m_{\mathrm{TC}} + a_{\mathrm{EA}} p_{\mathrm{a}}$. Note that only the $+\sqrt{\ldots}$ solution of (8b) is meaningful, since $-\Theta/c_{\mathrm{T}}$ in (8b) is strictly negative and u_{W} can only take positive values. Furthermore, the quantities Ψ, Θ, $\dot H_{\mathrm{TC}}$, c_{T}, and Υ are strictly positive by definition and due to the working principle of a turbine P_{T} is strictly positive as well. The control input u_{W} is thus uniquely defined for all admissible air system operating points. The obtained parametrizations

$$x = \Phi^{-1}(z) \quad \text{and} \quad u = \mu\big(z,\gamma\big)$$

as given by (4) and (8), respectively, can be used to compute the state x and the input u of the air system (2) from the flat output y and its time derivatives, combined in the vector

$$y^{[r]} = \left[\, y_1 \;\; \mathrm{d}y_1/\mathrm{d}t \;\; y_2 \;\; \mathrm{d}y_2/\mathrm{d}t \;\; \mathrm{d}^2y_2/\mathrm{d}t^2 \,\right]^{\mathrm{T}}.$$

The desired FF controller is easily obtained by replacing the vector $y^{[r]}$ in the parametrization (4), (8) with a corresponding vector $w^{[r]}$ of sufficiently smooth reference signals w_1 and w_2. Since the FF controller does not account for the input constraints $u \in \mathcal{U}$ according to (1), the TP generating the vector $w^{[r]}$ has to account for this.

IV. Constrained Trajectory Planning

The input constraints $u \in \mathcal{U}$ according to (1) are included into the control setup depicted in Fig. 1 via a constrained TP. Similar to model following control [25], [26], the desired tracking behavior for the controlled air system variables is at first defined by a linear target system in Sec. IV-A. The input constraints are taken into account by limiting the desired r-derivatives of the target system according to the priority of the corresponding air system outputs in Sec. IV-B. In particular, the set $\mathcal{U}$ of feasible inputs is transformed to the set $\Gamma = \gamma(\mathcal{U})$ of feasible r-derivatives, cf. (6), which is used to restrict the r-derivatives of the target system. As a consequence of the limitation, the constrained target system is a switched nonlinear dynamical system. Since the target system is, however, only limited if the desired behavior leads to a violation of the input constraints, the input space $\mathcal{U}$ is guaranteed to be fully exploited to achieve the best possible tracking performance. The implementation of the limited target system is finally simplified in Sec. IV-C.

A. Target-System-Based Trajectory Planning

In the unconstrained case, the desired tracking of the command input y^{d} by the plant output y, cf. Fig. 1, is defined by the reference signal w generated by the target system

$$\Sigma^{\mathrm{d}} : w = \mathrm{diag}\left(\Sigma_1^{\mathrm{d}}, \Sigma_2^{\mathrm{d}}\right) y^{\mathrm{d}}, \tag{9a}$$

which is composed of two independent dynamical systems

$$\Sigma_i^{\mathrm{d}} : \begin{cases} \dfrac{\mathrm{d}\xi_{i,j}}{\mathrm{d}t} = \xi_{i,j+1}, \; j = 1,\ldots,r_i - 1 \\[2mm] \dfrac{\mathrm{d}\xi_{i,r_i}}{\mathrm{d}t} = \gamma_i^{\mathrm{d}}\big(\xi_i, y_i^{\mathrm{d}}\big) \\[2mm] w_i = \xi_{i,1} \end{cases}, \; i = 1,2 \tag{9b}$$

Post-print version of the article: P. Kotman, M. Bitzer, and A. Kugi, "Prioritization-based constrained trajectory planning for a nonlinear turbocharged air system with EGR", in *Proccedings of the American Control Conference (ACC)*, Montreal, Canada, Jun. 2012, pp. 5712–5717
The content of this post-print version is identical to the published paper but without the publisher's final layout or copy editing.

with states $\xi_i \in \mathbb{R}^{r_i}$, inputs $y_i^{\mathrm{d}} \in \mathbb{R}$, and outputs $w_i \in \mathbb{R}$. The state of the overall target system Σ^{d} is further defined by $\xi = [\xi_{1,1}\ \ \xi_{2,1}\ \ \xi_{2,2}]^{\mathrm{T}}$. A common choice for the target systems Σ_i^{d} are r_i-th order lag elements, realized by

$$\gamma_i^{\mathrm{d}}(\xi_i, y_i^{\mathrm{d}}) = \frac{1}{T_i^{r_i}}\left(y_i^{\mathrm{d}} - \sum_{k=1}^{r_i}\binom{r_i}{k}T_i^{r_i-k}\xi_{i,r_i-k+1}\right) \tag{9c}$$

with time constants $T_i > 0$. The control input u obtained from the parametrization (4), (8) on the basis of the vector

$$w^{[r]} = \left[\,\xi_{1,1}\ \mathrm{d}\xi_{1,1}/\mathrm{d}t\ \xi_{2,1}\ \ \xi_{2,2}\ \mathrm{d}\xi_{2,2}/\mathrm{d}t\,\right]^{\mathrm{T}} \tag{9d}$$

achieves the desired tracking. That is, the output y of the air system (2) tracks the command input y^{d} in exact the same way as the output w of the target system (9).

The parametrization (4), (8) and its inverse (5), (6) define an invertible transformation between the state ξ and input y^{d} of the target system Σ^{d} (9) and the state x and input u of the air system Σ (2). The target system Σ^{d} and the air system Σ are thus said to be differentially equivalent [27], which is however only true if the corresponding input u obtained on the basis of $w^{[r]}$ (9d) satisfies the input constraints (1), i.e.

$$u^{\mathrm{d}} = \mu\Big(\xi, \gamma_1^{\mathrm{d}}(\xi_1, y_1^{\mathrm{d}}), \gamma_2^{\mathrm{d}}(\xi_2, y_2^{\mathrm{d}})\Big) \in \mathcal{U}\ \ \forall\ \xi, y_1^{\mathrm{d}}, y_2^{\mathrm{d}}. \tag{10}$$

To this end, a limitation of the desired r-derivatives γ_i^{d} generated by the target systems Σ_i^{d} is developed next.

B. Prioritization-Based Target System Limitation

In order to guarantee that the constraint equation (10) is always fulfilled, a limitation of the target system (9) is required. Thereby, the only quantities that can be changed for this purpose are the desired r-derivatives γ_i^{d}.

The idea of the prioritization-based approach is to perform this limitation of the desired r-derivatives γ_i^{d} according to the priority of the corresponding outputs y_i. In particular, the r-derivative γ_1 of the most important output y_1 has to be as close to its desired value γ_1^{d} as possible while the constraints $u \in \mathcal{U}$ are satisfied. Mathematically speaking, the respectively limited r-derivative $\gamma_1^{\mathrm{l}} = \gamma_1(x^{\mathrm{d}}, u^*)$ is defined on the basis of the minimizer u^* of the optimization problem

$$\min_{u\in\mathcal{U}}\ \left|\gamma_1^{\mathrm{d}}(\xi, y^{\mathrm{d}}) - \gamma_1(x^{\mathrm{d}}, u)\right|, \tag{11}$$

with $x^{\mathrm{d}} = \Phi^{-1}(\xi)$, cf. (4). Since (11) is a scalar optimization problem, the limited r-derivative γ_1^{l} can as well be obtained by saturating the desired r-derivative γ_1^{d} according to

$$\gamma_1^{\mathrm{l}} = \mathrm{sat}\big(\gamma_1^{\mathrm{d}}, \underline{\gamma}_1, \overline{\gamma}_1\big) = \begin{cases} \underline{\gamma}_1 & \text{if} \quad \gamma_1^{\mathrm{d}} < \underline{\gamma}_1 \\ \gamma_1^{\mathrm{d}} & \text{else} \\ \overline{\gamma}_1 & \text{if} \quad \gamma_1^{\mathrm{d}} > \overline{\gamma}_1 \end{cases} \tag{12}$$

where

$$\underline{\gamma}_1 = \min_{u\in\mathcal{U}}\ \gamma_1(x^{\mathrm{d}}, u), \quad \overline{\gamma}_1 = \max_{u\in\mathcal{U}}\ \gamma_1(x^{\mathrm{d}}, u). \tag{13}$$

In a second step, the difference between the r-derivative γ_2 and the corresponding desired value γ_2^{d} is minimized, while the result $\gamma_1(x^{\mathrm{d}}, u) = \gamma_1^{\mathrm{l}}$ obtained in the first step has to be preserved. As in the previous step, the value of γ_2 that is closest to the corresponding desired value γ_2^{d} is

$$\gamma_2^{\mathrm{l}} = \mathrm{sat}\big(\gamma_2^{\mathrm{d}}, \underline{\gamma}_2, \overline{\gamma}_2\big), \tag{14}$$

i.e. the saturated desired r-derivative γ_2^{d}, where

$$\underline{\gamma}_2 = \min_{\substack{u\in\mathcal{U} \\ \text{s.t. } \gamma_1(x^{\mathrm{d}},u)=\gamma_1^{\mathrm{l}}}}\ \gamma_2(x^{\mathrm{d}}, u), \qquad \overline{\gamma}_2 = \max_{\substack{u\in\mathcal{U} \\ \text{s.t. } \gamma_1(x^{\mathrm{d}},u)=\gamma_1^{\mathrm{l}}}}\ \gamma_2(x^{\mathrm{d}}, u). \tag{15}$$

Note that (13) defines two static optimization problems constrained by $u \in \mathcal{U}_1 = \mathcal{U}$ only, while the two problems in (15) are constrained by $u \in \mathcal{U}_2 = \mathcal{U} \cap \{u|\gamma_1(x^{\mathrm{d}}, u) = \gamma_1^{\mathrm{l}}\}$, where $\gamma_1(x^{\mathrm{d}}, u) = \gamma_1^{\mathrm{l}}$ preserves the achieved tracking for γ_1.

In Fig. 3, the determination of a limited control input $u^{\mathrm{l}} = \mu(\xi, \gamma_1^{\mathrm{l}}, \gamma_2^{\mathrm{l}})$ by means of the prioritization-based limitation L_{PB} is exemplified. There, the desired r-derivative γ^{d} leading to the infeasible control input u^{d} is restricted to the limited r-derivative γ^{l} resulting in the feasible input u^{l}.

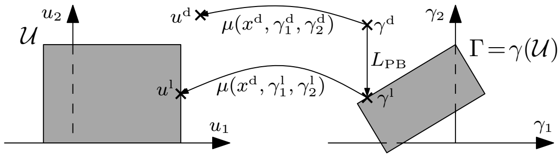

Fig. 3. Example for the prioritization-based target system limitation L_{PB}.

The detailed control structure obtained on the basis of the previous results is depicted in Fig. 4. Thereby, $1/s^r$ denotes the parallel connection of the r_i-th order chains of integrators used in the definition of the target systems Σ_i^{d} (9b). Furthermore, the vector $w^{[r]}$, cf. (9d) and see Fig. 4, is composed of the state ξ of the target system (9) and the limited r-derivatives γ_1^{l} (12) and γ_2^{l} (14).

C. Simplified Implementation for Air System Control

Finally, the implementation of the constrained target system is simplified in order to avoid the numerical online-solution of the optimization problems in (13) and (15). For this, the limits $\underline{\gamma}_i$ and $\overline{\gamma}_i$ in (12) and (14) are determined analytically. More precisely, the LAGRANGE-functions [28]

$$L_1(u) = \gamma_1(x^{\mathrm{d}}, u) \tag{16a}$$

$$L_2(u, \lambda) = \gamma_2(x^{\mathrm{d}}, u) + \lambda\left(\gamma_1(x^{\mathrm{d}}, u) - \gamma_1^{\mathrm{l}}\right) \tag{16b}$$

of the optimization problems (13) and (15), where λ is the LAGRANGE-multiplier, are proven to be strictly monotonic with respect to the control input u within $\mathcal{U}_1$ and $\mathcal{U}_2$, respectively. Hence the corresponding minimizers u^* have

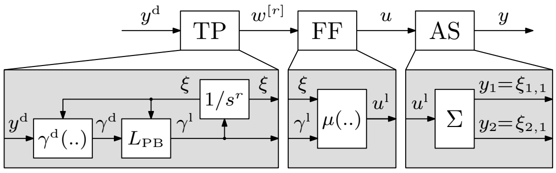

Fig. 4. Detailed setup used for air system control, with a prioritization-based trajectory planning and a flatness-based feedforward controller.

Post-print version of the article: P. Kotman, M. Bitzer, and A. Kugi, "Prioritization-based constrained trajectory planning for a nonlinear turbocharged air system with EGR", in *Proccedings of the American Control Conference (ACC)*, Montreal, Canada, Jun. 2012, pp. 5712–5717

to be located on the vertices of the constraint sets $\mathcal{U}_1$ and $\mathcal{U}_2$. To do so, the necessary conditions of optimality [28]

$$\frac{\partial L_1}{\partial u_{\mathrm{E}}} = 0, \quad \frac{\partial L_1}{\partial u_{\mathrm{W}}} = 0, \tag{17a}$$

$$\text{and} \quad \frac{\partial L_2}{\partial u_{\mathrm{E}}} = 0, \quad \frac{\partial L_2}{\partial u_{\mathrm{W}}} = 0, \quad \frac{\partial L_2}{\partial \lambda} = 0, \tag{17b}$$

for the optimization problems in (13) and (15), respectively, are solved for the inputs u_{E} and u_{W}. For both, (17a) and (17b), this either leads to

$$u_{\mathrm{E}} = \frac{-\dot{m}_{\mathrm{E}}}{a_{\mathrm{EV}}\Delta p_{\mathrm{a}}}, \text{ or } u_{\mathrm{W}} = \frac{-1}{c_{\mathrm{T}}}\left(\frac{a_{\mathrm{EA}}\dot{m}_{\mathrm{E}}}{\dot{m}_{\mathrm{E}} - a_{\mathrm{EA}}\Delta p_{\mathrm{a}}} + \Theta\right), \tag{18}$$

while the respective other control input can be chosen arbitrarily. Both expressions in (18) are strictly negative for all admissible operating points of the air system and thus all solutions to (17) involve control inputs violating the input constraints $u \in \mathcal{U}$. The minimum and maximum air system r-derivatives $\underline{\gamma}_i$ and $\overline{\gamma}_i$ required for the limitation of the target system r-derivatives γ_i^{d} according to (12) and (14) therefore have to be located on the vertices of the corresponding constraint set $\mathcal{U}_i$. They can hence be determined by evaluating the r-derivatives γ_i (6) on the vertices of the corresponding constraint sets $\mathcal{U}_i$ instead of solving the nonlinear inequality constrained optimization problems in (13) and (15).

In conclusion, the desired constrained TP is defined as a linear target system which is limited by a prioritization-based approach. Although the prioritization involves nonlinear optimization problems, the constrained target system can be implemented in a numerically efficient way avoiding the numerical solution of these optimization problems. Due to the prioritization-based limitation, the obtained TP is a switched nonlinear system featuring linear input-output dynamics in the unlimited case, cf. (9). In the limited case, the input-output dynamics of the TP is defined by the maximum achievable dynamics of the air system, i.e. by replacing the desired linear r-derivative γ_i^{d} in the definition of the target system Σ_i^{d} (9b) by the corresponding r-derivative γ_i of the nonlinear air system model in accordance to (6).

A systematic rigorous proof of stability for the switching nonlinear TP is a challenging task and still an open problem. Extensive simulation studies, however, indicate a large region of stability of the TP in terms of the design parameters T_i, i.e. the time constants of the target systems Σ_i^{d} (9b).

V. Simulation Results

The suitability of the developed control structure, see Fig. 4, is tested by means of simulation studies in this section. In particular, a stationary evaluation of the ROM (2) is presented in Sec. V-A. The combination of the FF controller and the constrained TP is evaluated in Sec. V-B.

A. Evaluation of the Reduced-Order Model

A stationary evaluation of the approximation performance of the ROM (2) with respect to the FOM from [22] is depicted in Fig. 5, where the approximation errors δr_{E} and δp_2 of the EGR rate r_{E} and the boost pressure p_2, respectively,

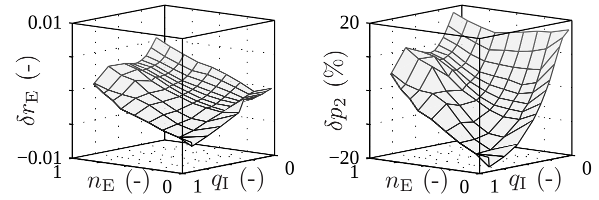

Fig. 5. Approximation performance of the ROM (2) with respect to the FOM from [22]. Left: EGR rate error δr_{E}. Right: boost pressure error δp_2.

are presented by means of scaled quantities. It can be inferred from Fig. 5 that, considering the significant simplifications achieved in the course of the model reduction, the ROM (2) features an excellent approximation performance.

B. Prioritization-Based Constrained Trajectory Planning

The tracking performance of the developed control setup with respect to the FOM is tested by means of the simulation study depicted in Fig. 6. Thereby, the external signals, i.e. the engine speed n_{E} and the injected fuel mass q_{I}, are given in the bottom plot. In the first and second plot, the corresponding command inputs $r_{\mathrm{E}}^{\mathrm{d}}$ and p_2^{d} are compared to the smooth reference signals $r_{\mathrm{E}}^{\mathrm{p}}$ and p_2^{p} generated by the TP and the outputs r_{E} and p_2 of the FOM of the air system, respectively. Thereby, the command inputs $r_{\mathrm{E}}^{\mathrm{d}}$ and p_2^{d} are determined by the current engine speed n_{E} and the injected fuel mass q_{I}. The control inputs u_{E} and u_{W} computed by the FF controller are depicted in the third plot of Fig. 6. At this point it is furthermore important to stress that the presented results are generated without using any feedback (FB) controller. Note that the results are presented by means of scaled quantities.

First of all, the presented results show the suitability of the air system control setup depicted in Fig. 4. That is,

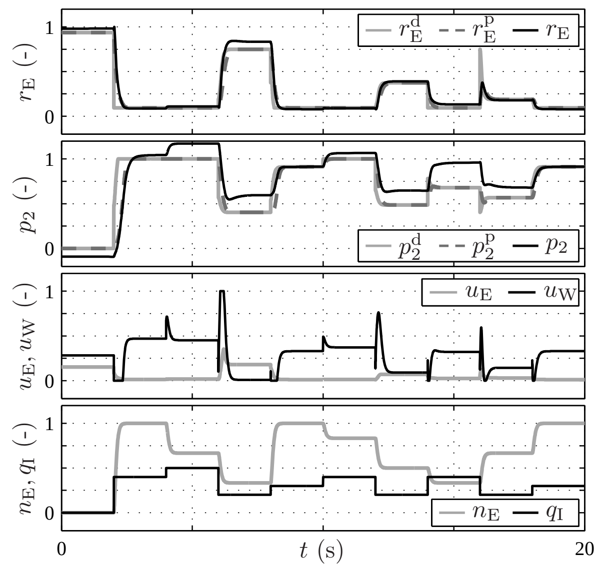

Fig. 6. Simulation results for air system control with prioritization-based trajectory planning and flatness-based feedforward controller (full).

Post-print version of the article: P. Kotman, M. Bitzer, and A. Kugi, "Prioritization-based constrained trajectory planning for a nonlinear turbocharged air system with EGR", in *Proccedings of the American Control Conference (ACC)*, Montreal, Canada, Jun. 2012, pp. 5712–5717
The content of this post-print version is identical to the published paper but without the publisher's final layout or copy editing.

considering that no FB control is used, a good tracking performance for the EGR rate r_E and the boost pressure p_2 is achieved, and furthermore the multivariable behavior of the system is indeed taken into account by the controller.

From the first two plots it can be seen that the smooth reference signals r_E^p and p_2^p (gray solid lines) generated by the TP track the respective command inputs r_E^d and p_2^d (gray dashed lines) with no steady-state offset. Furthermore, the stability of the TP can be inferred for the operational range of the engine covered by the presented simulation study. Finally, the stipulated limitation $u \in \mathcal{U}$ according to (1) of the control input is obviously achieved by the constrained TP.

A more detailed view of the first transient around $t = 4$ s is given in Fig. 7. For clarity, the lower limit $\underline{u}_\mathrm{E} = \underline{u}_\mathrm{W} = 0$ is shown by the dashed line. It can be seen that the available range $0 \leq u_\mathrm{W} \leq \overline{u}_\mathrm{W}$ for the wastegate actuation u_W is indeed fully exploited to achieve the desired tracking.

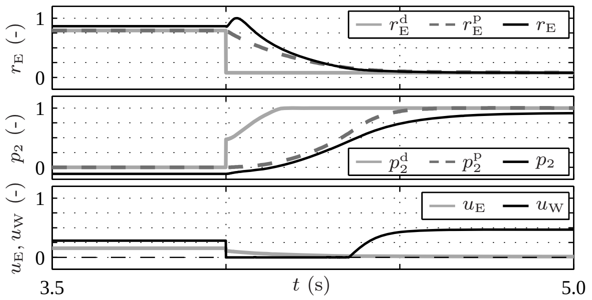

Fig. 7. Simulation results for air system control with prioritization-based trajectory planning and flatness-based feedforward controller (detail).

VI. Conclusion & Outlook

In this work, a constrained trajectory planning (TP) generating the smooth reference signal required by a flatness-based feedforward (FF) air system controller is presented. It accepts arbitrary command inputs and determines the reference signal in such a way that the available input space is fully exploited to achieve the best possible performance in terms of tracking fast reference trajectories. The TP is based on a linear target system in accordance to the ideas of model reference control. In order to account for the input constraints of the air system the target system is limited using a prioritization-based approach, thus allowing for a systematic prioritization of the controlled variables. As a consequence of the chosen structure, i.e. a linear target system limited by a prioritization-based approach, the obtained TP is a switched nonlinear dynamical system. The systematic proof of the stability as well as the evaluation of alternative limitation techniques are the topic of future research activities. The presented TP is furthermore adopted for the control of a two-stage turbocharged air system with EGR.

Finally, in order to robustify the control setup with respect to model uncertainties and disturbances the developed FF control setup has to be completed by a feedback controller.

References

[1] L. Guzzella and C. H. Onder, *Introduction to Modeling and Control of Internal Combustion Engine Systems*, 2nd ed. Springer, 2010.

[2] A. G. Stefanopoulou, I. Kolmanovsky, and J. S. Freudenberg, "Control of variable geometry turbocharged diesel engines for reduced emissions," *IEEE T. Contr. Syst. T.*, vol. 8, no. 4, pp. 733–745, July 2000.

[3] M. Herceg, T. Raff, R. Findeisen, and F. Allgöwer, "Nonlinear Model Predictive Control of a Turbocharged Diesel Engine," in *Proc. IEEE Conf. Contr. Appl.*, Munich, Germany, 2006, pp. 2766–2771.

[4] A. Plianos and R. Stobart, "Dynamic feedback linearization of Diesel engines with intake variable valve actuation," in *Proc. IEEE Conf. Contr. Appl.*, Singapore, 2007, pp. 455–461.

[5] A. Saberi, A. A. Stoorvogel, and P. Sannuti, *Control of linear systems with regulation and input constraints*. Springer, 2003.

[6] P. Hippe, *Windup in Control*. Springer, 2006.

[7] P. Ortner and L. Del Re, "Predictive Control of a Diesel Engine Air Path," *IEEE T. Contr. Syst. T.*, vol. 15, no. 3, pp. 449–456, May 2007.

[8] J. Chauvin, G. Corde, N. Petit, and P. Rouchon, "Motion planning for experimental airpath control of a diesel homogeneous charge-compression ignition engine," *Contr. Eng. Pract.*, vol. 16, pp. 1081–1091, 2008.

[9] V. Kapila and K. M. Grigoriadis, *Actuator Saturation Control*. Marcel Dekker, Inc., 2002.

[10] J. C. Dolye, R. S. Smith, and D. F. Enns, "Control of Plants with Input Saturation Nonlinearities," in *Proc. Am. Contr. Conf.*, Minneapolis, MN, USA, 1987, pp. 1034–1039.

[11] M. Soroush and S. Valluri, "Optimal directionality compensation in processes with input saturation non-linearities," *Int. J. Contr.*, vol. 72, no. 7, pp. 1555–1564, 1999.

[12] S. Tarbouriech, G. Garcia, and A. H. Glattfelder, *Advanced Strategies in Control Systems with Input and Output Constraints*. Springer, 2007.

[13] M. Janković, M. Janković, and I. Kolmanovsky, "Constructive Lyapunov Control Design for Turbocharged Diesel Engines," *IEEE T. Contr. Syst. T.*, vol. 8, no. 2, pp. 288–299, March 2000.

[14] D. Upadhyay, V. I. Utkin, and G. Rizzoni, "Multivariable Control Design for Intake Flow Regulation of a Diesel Engine using Sliding Mode," in *Proc. IFAC World Cong.*, Barcelona, Spain, 2002.

[15] J. F. Arnold, N. Langlois, H. Chafouk, and G. Trémoulière, "Control of the air system of a diesel engine: A fuzzy multivariable approach," in *Proc. IEEE Conf. Contr. Appl.*, Munich, Germany, 2006, pp. 2132–2137.

[16] M. Jung and K. Glover, "Calibratable Linear Parameter-Varying Control of a Turbocharged Diesel Engine," *IEEE T. Contr. Syst. T.*, vol. 14, no. 1, pp. 45–62, January 2006.

[17] S. García-Nieto, M. Martínez, X. Blasco, and J. Sanchis, "Nonlinear predictive control based on local model networks for air management in diesel engines," *Contr. Eng. Pract.*, vol. 16, pp. 1399–1413, 2008.

[18] M. Fliess, J. Lévine, P. Martin, and P. Rouchon, "Flatness and defect of nonlinear systems: introductory theory and examples," *Int. J. of Control*, vol. 61, pp. 1327–1361, 1995.

[19] P. Kotman, M. Bitzer, and A. Kugi, "Flatness-Based Feedforward Control of a Diesel Engine Air System with EGR," in *Proc. IFAC Symp. Adv. in Automot. Contr.*, Munich, Germany, 2010.

[20] G. Ambrosino, G. Celentano, and F. Garofalo, "Robust Model Tracking Control for a Class of Nonlinear Plants," *IEEE T. Automat. Contr.*, vol. 30, no. 3, pp. 275–279, 1985.

[21] C. D. Onal and A. Sabanovic, "Plant Behaviour Dictation using a Sliding Mode Model Reference Controller," in *Proc. IEEE Workshop Adv. Mot. Contr.*, Istanbul, Turkey, 2006, pp. 243–248.

[22] P. Kotman, M. Bitzer, K. Graichen, and A. Kugi, "Hybrid Modeling of a Two-Stage Turbocharged Diesel Engine Air System," in *Proc. Vienna Symp. Math. Mod.*, Vienna, Austria, 2009, pp. 2015–2024.

[23] H. K. Khalil, *Nonlinear Systems*, 3rd ed. Prentice-Hall, 2000.

[24] A. Isidori, *Nonlinear Control Systems*, 3rd ed. Springer, 1995.

[25] A. S. Morse, "Structure and Design of Linear Model Following Systems," *IEEE T. Automat. Contr.*, vol. 18, no. 4, pp. 346–354, 1973.

[26] J. R. Broussard and P. W. Berry, "The Relationship Between Implicit Model Following and Eigenvalue Eigenvector Placement," *IEEE T. Automat. Contr.*, vol. 25, no. 3, pp. 591–594, 1980.

[27] M. Fliess, J. Lévine, P. Martin, and P. Rouchon, "A Lie-Bäcklund Approach to Equivalence and Flatness of Nonlinear Systems," *IEEE T. Automat. Contr.*, vol. 44, no. 5, pp. 922–937, 1999.

[28] J. Nocedal and S. J. Wright, *Numerical Optimization*, 2nd ed. Springer, 2006.

Post-print version of the article: P. Kotman, M. Bitzer, and A. Kugi, "Prioritization-based constrained trajectory planning for a nonlinear turbocharged air system with EGR", in *Proccedings of the American Control Conference (ACC)*, Montreal, Canada, Jun. 2012, pp. 5712–5717
The content of this post-print version is identical to the published paper but without the publisher's final layout or copy editing.